



FEBS Letters

journal homepage: www.FEBSLetters.org



Theoretical mimicry of biomembranes

Parimal Kar^a, Max Seel^a, Thomas Weidemann^b, Siegfried Höfner^{a,c,*}

^a Department of Physics, Michigan Technological University, 1400 Townsend Drive, Houghton, MI 49931-1295, USA

^b Institute of Biophysics, Biotechnologisches Zentrum der TU Dresden, Biotec, Tatzberg 47-51, D-01307 Dresden, Germany

^c Dipartimento di Chimica "G. Ciamician", Università di Bologna, Via F. Selmi 2, 40126 Bologna, Italy

ARTICLE INFO

Article history:

Received 11 February 2009

Revised 3 April 2009

Accepted 23 April 2009

Available online 3 May 2009

Edited by Robert B. Russell

Keywords:

Biomembrane

Membranous environment

Mimicry solvent

Polarizable continuum method

ABSTRACT

The study of membrane proteins requires a proper consideration of the specific environment provided by the biomembrane. The compositional complexity of this environment poses great challenges to all experimental and theoretical approaches. In this article a rather simple theoretical concept is discussed for its ability to mimic the biomembrane. The biomembrane is approximated by three mimicry solvents forming individual continuum layers of characteristic physical properties. Several specific structural problems are studied with a focus on the biological significance of such an approach. Our results support the general perception that the biomembrane is crucial for correct positioning and embedding of its constituents. The described model provides a semi-quantitative tool of potential interest to many problems in structural membrane biology.

© 2009 Federation of European Biochemical Societies. Published by Elsevier B.V. All rights reserved.

1. Introduction

All living cells maintain a barrier between what is considered self and what is considered outside world. Biomembranes constitute the physical medium of this barrier and all of the incoming and outgoing signals need to be transmitted over this barrier via specifically designed receptors. Biomembranes therefore establish a semipermeable border that is vital to the cell. This central role of biomembranes is reflected also in the industrial interest in this particular domain. A considerable fraction of current drug discovery efforts is focused on membrane proteins and related phenomena [1]. Consequently, learning and understanding the fundamental principles that govern the physico-chemical interaction in biomembranes is of crucial interest to a mechanistic understanding of membrane-embedded receptors (which in turn is key to a successful interference by any type of medicine).

Abbreviations: PH, polar headgroup domain of the biomembrane; HC, hydrophobic core domain of the biomembrane; AQ, aqueous domains above and below the biomembrane; PCM, polarizable continuum method; BEM, boundary element method; PDBTM, database for membrane proteins; 2CPS, 1JDM, 2HAC, pdb codes of 3 membrane proteins; TM, transmembrane domain; MP, membrane protein; NMR, nuclear magnetic resonance; AMBER, a molecular mechanics program and force field; MD, molecular dynamics; rmsd, root mean square deviation

* Corresponding author. Address: Dipartimento di Chimica "G. Ciamician" Università di Bologna, Via F. Selmi 2, 40126 Bologna, Italy. Fax: +39 051 209/9456.

E-mail addresses: siegfried.hoefner@unibo.it, shoefing@mtu.edu (S. Höfner).

A striking characteristics of biomembranes is their sudden change in polarity and dielectric properties [2–4]. In fact, already early attempts of describing the basic behaviour of membrane-bound processes have tried to employ just this basic feature [5]. The approximation being made is to drop all atomic level of detail and consider the biomembrane as a uniform dielectric medium of low dielectric constant ($\epsilon \approx 2$). Despite the rather crude nature of such a model, the most essential features of biomembranes seem to be retained by such a continuum approach [6–9]. Of course, many membrane-related problems will need a more detailed picture—sometimes of even atomic resolution [10–12]. However, a large body of conformational studies and problems concerning energetic preference of membrane exposed orientations may be described sufficiently well by such a simplistic continuum picture of the lipid bilayer [13–15]. The present work builds on the continuum approximation but will extend it as follows, (i) a refined composition into three layers of dielectric continua will be used, (ii) a more complete physical description for each individual continuum will be employed, (iii) the combined action of each individual continuum on an embedded protein will be brought together smoothly via the boundary element method, and (iv) an efficient computing scheme will be applied.

When stating “*experiment is the sole judge of scientific truth*” Richard Feynman has made it all clear that all theoretical efforts need experimental verification [16]. Biological assays will have to provide the test-bed for studies involving biomembranes and the level of appreciation of the theory will strongly depend on the

accuracy and versatility of the model to reproduce experimental findings. In the following a series of such biological problems will be addressed by a continuum description of biomembranes. Different aspects of biochemical importance will be examined and analyzed in detail. The focus is entirely on the biological relevance of the approach rather than on methodic details. A picture is emerging that strongly supports the usefulness of the presented concept with likely impact on routine practice in the biochemical laboratory.

2. Materials and methods

2.1. Theoretical concepts

A multiple continua approach is adopted to describe the biomembrane. Three different regions of distinct physical properties are considered. Correspondingly, three different mimicry solvents serve for the description of these domains. The experimentally determined dielectric constant representative of a particular domain inside the biomembrane [3] guides the selection process for these solvents. Ethanol is used to represent the polar head-group (PH) domain of the biomembrane (see Fig. 2). This also includes the acetyl region [3] and is estimated to spawn a 10 Å thick layer at the aqueous interface of the biomembrane. A 30 Å thick interior domain is allocated for the hydrophobic core region (HC) of the biomembrane and cyclohexane is employed for its representation. The adjacent aqueous domains (AQ) are also included via a continuum description of water. An enhanced Poisson–Boltzmann description is used for each of the model solvents [17]. The theoretical framework is based on the polarizable continuum method (PCM) [18], hence the solvation/environmental free energy may be split into three major partial contributions,

$$\Delta G^{\text{sol}/\text{env}} = \Delta G^{\text{pol}} + \Delta G^{\text{cav}} + \Delta G^{\text{disp}} \quad (1)$$

that account for polarization [19], cavitation [20] and dispersion effects [17]. The boundary element method (BEM) [21] allows each of these three effects to be expressed with respect to individual boundary elements. Consequently, different boundary elements may be assigned to different domains of the biomembrane. Since the latter are represented by specific mimicry solvents, the simple generalization achieved here is to allow each of the boundary elements to choose their parameterization from the list of available mimicry solvents. Let us consider a single-spanning membrane protein as depicted in Fig. 2. The protein is simultaneously exposed to all various domains of the biomembrane as well as to the adjacent aqueous domain. The aforementioned multiple continua approach will account for such a situation by (i) assigning specific membrane domain exposure to different parts of the protein, (ii) computing a piecewise homogeneous boundary composed of BEs that are characteristic of a particular mimicry solvent, (iii) solving Eq. (1) in a compound fashion with simultaneous consideration of all types of different interactions. In this context it is important to realize that the above problem is not a simple sum of separated subproblems (for different solvents) but merely a complex problem with mutual interaction between each of the individual subdomains. A PCM-like decomposition of such a multiple continua approach is particularly advantageous since it facilitates a formally correct distinction of individual boundary sections. Widely used surface area models are problematic in this respect. A more detailed description of the underlying theoretical concept is given in the [Supplementary material](#) (Sections 1.1–1.3 for individual terms of Eq. (1), Section 1.4 for generalization to multiple continua, Table I to summarize model parameters).

2.2. Sample selection and preparation

Protein structure coordinates of representative examples were downloaded from the repository PDBTM [22] (pdb codes, 2CPS, 1JDM, 2HAC). The most representative structure was selected from the nuclear magnetic resonance (NMR) ensembles. AMBER parameters [23] (a molecular mechanics program and force field) were assigned using adjustment parameters as summarized in [Table I of the Supplementary material](#). N- and C-terminal ends of transmembrane domains (TM) were selected by marking positions of C_{α} atoms of the initial/final turns and computing the geometric centre thereof. The TM-centre was calculated as the midpoint in between these two terminal ends. Bent membrane protein structures and more complicated geometries would obviously require a different protocol. The vector describing the TM-axis is computed similarly and normalized. Knowledge of these two parameters is sufficient to define the midplane of the biomembrane. Distances for any arbitrary point away from this midplane can be computed straightforwardly. C_{α} atoms of all residues of the selected sample structures were examined and distances to the midplane computed in direction perpendicular to the midplane. The corresponding membrane domain was assigned following Ashcroft et al. [3]. Solvents ethanol, cyclohexane and water served for biomembrane mimicry of domains PH, HC and AQ, respectively. Simple geometric transformations such as translations along the TM-axis or rotations around it were carried out using standard scripting techniques. Program POLCH [19] was used for all multiple continua calculations following the framework described in the [Supplementary material](#). In addition to TM-domains simple organic molecules, i.e. H_2O , NH_3 and O_2 , were probed for biomembrane insertion experiments as reported by Berendsen and coworkers [10–12]. Parameterization of these small molecules was done similarly to the process described previously [17]. The influence of conformational variability was partially addressed in the test carried out with sample 1JDM. Here the main experiment was repeated several times using a set of 35 different conformations instead of the single static pdb structure. The 35 different 1JDM conformations were generated from a short term molecular dynamics simulation (MD) recorded at standard conditions in explicit solvent. The small subset of conformations was selected based on the root mean square deviation (rmsd) value which was required not to exceed 2 Å when compared to the original pdb structure. More extensive ensembles would have increased the fraction of non-natural conformations that deviate severely from the experimental geometry.

2.3. Re-computing the experimental hydrophobicity scale of Wimley and White

The same set of peptides used in the Wimley–White experiment [24] was model-constructed with program PROTEIN from the TINKER package [25]. N-terminal acetyl groups were employed while the C-terminal end was unprotected, hence carried a negative charge. The basic pattern reads Ac-WL-X-LL in single letter amino acid code. The variable X represents any of the 20 different types of amino acids under investigation. The second subset of AcWL_m peptides with m ranging from 1 to 5 was constructed similarly. All model peptides were placed in solvent boxes (using explicit water), minimized and equilibrated to room temperature. 1 ns MD simulations were then carried out using standard protocols and package AMBER [23]. One hundred snapshots of intermediate configurations were saved and the solvent molecules discarded (used only to provide a more reasonable environment and prevent internal structural collapse). Each of the 100 snapshot structures for all the 20 different types of amino acids (and the additional AcWL_m series) were then considered within the multiple continua approach using all three types of mimicry solvents representative

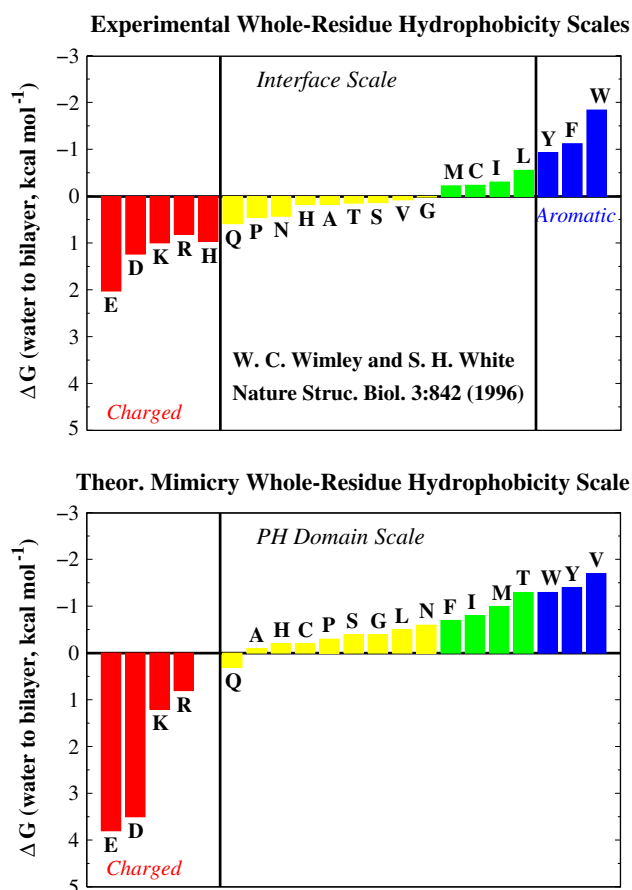


Fig. 1. Comparison of the experimentally determined hydrophobicity scale (Wimley and White) to theoretical results obtained with mimicry solvents using a multiple continua approach. Details are given in the text and in Ref. [24]. The theoretical data resemble the experimental results rather closely. The ranking order is perfectly reproduced for the charged residues and qualitatively comparable for the remainder (minor exceptions V and T). Even semi-quantitative agreement between experimental and theoretical scale may be claimed.

of the AQ, PH and HC domains. Average net solvation free energies were computed for all samples and the two Wimley–White relations employed (see Fig. 1 and Eq. (1a) in Ref. [24]). Interface partitioning free energies are computed as $\Delta G_{WLXLL} = \Delta G_{WLXLL}^{env/PA} - \Delta G_{WLXLL}^{env/AQ}$ and individual terms represent average free energies.

3. Results and discussion

In order to evaluate the multiple continua approach, we chose four examples involving short peptides and small membrane spanning proteins (MP). Experimentally determined NMR structures for the latter class were available. The individual examples classify four main problems:

- what is the preferred domain for different types of amino acids when having the choice between the aqueous (AQ) and the membrane interface domain (PH);
- what is the favoured vertical position of a TM segment;
- how are MP-subdomains arranged with respect to each other;
- how are non-covalently formed dimers oriented within their complex.

3.1. The experimentally determined hydrophobicity scale of Wimley and White [24] is largely reproduced by the multiple continua approach using mimicry solvents for representation of the biomembrane

In a rather prominent experiment Wimley and White have tested the tendency of all 20 different types of amino acids to migrate into the bilayer interface [24]. Short structureless pentapeptides were employed and a series of ascending hydrophobicities was established ranking each individual type of amino acid according to its tendency to migrate into the bilayer interface. A graphical representation of the Wimley/White scale is shown in Fig. 1 (upper panel). The same set of pentapeptides was also considered within the multiple continua approach. To account for conformational flexibility short runs of MD simulations were carried out and 100 snapshots were saved for each different type of pentapeptide. An identical evaluation scheme was followed as described in the original Wimley/White article [24]. Partitioning free energies are computed here as

$$\Delta G_{WLXLL}^{(PH)-(AQ)} = \Delta G_{WLXLL}^{(AQ)} - \Delta G_{WLXLL}^{(PH)} \quad (2)$$

with PA and AQ indicating the residence domain, i.e. either aqueous or polar headgroup domain of the biomembrane, where the latter is exactly the region probed by the Wimley/White experiment. WLXLL explains the composition of the host–guest peptides and X stands for any of the 20 types of amino acids under investigation. Mimicry solvents are water (AQ) and ethanol (PH). The theoretically computed hydrophobicity scale is also shown in Fig. 1 (lower panel). Corresponding free energies are summarized in Table II of Supplementary material. The theoretical results resemble the experimental results rather closely. The order is largely reproduced with particular success for charged residues and a high level of agreement for the remainder (notable exceptions V and T). Even semi-quantitative accuracy is achieved. The current results support the principal usefulness of a theoretical method like the multiple continua approach. The agreement to the Wimley/White experiment emphasizes the conceptual importance of including an extra layer for the interface domain (PH). A further remarkable signature of methodic strength is revealed when carefully analyzing the partial contributions of the different terms shown in Eq. (1). Detailed data are provided in Table III of the Supplementary material for two examples on either end of the Wimley/White scale. The important aspect to notice is the change in sign of transfer free energies—a crucial requirement for successful reconstruction of the Wimley/White scale.

This change in sign can only be facilitated by significantly varying contributions of the non-polar terms, ΔG^{cav} and ΔG^{disp} . Commonly employed SASA models are too insensitive to establish similar levels of accuracy. It is important to note that the current results are achieved without any re-adjustment of internal parameters. All mimicry solvents have been parameterized stand-alone on separate data sets and when applied in compound fashion within the multiple continua approach default parameters of the individual mimicry solvents are used.

3.2. The vertical biomembrane insertion profile of a single-spanning MP highlights mechanisms of membrane integration

α -Helical structure was reported for sarcolipin [26], a single-spanning membrane protein regulating Ca^{2+} -release in the context of skeletal muscle contraction. Vertical insertion of sarcolipin into the bilayer is probed via a multiple continua approach where various degrees of insertion are considered individually (see Fig. 2). The resulting ΔG^{env} profile is shown in Fig. 2. The shape of the obtained ΔG^{env} profile is very symmetric. This implies that the amino

acid sequence is not the decisive factor for the vertical insertion process. The optimal location is found in the middle of the bilayer when the TM-helix is fully integrated. Shifting terminal ends into either direction away from this position would result in an energy penalty. Similarly, inserting the tips of the TM from either site into the membrane is energetically disfavoured up to a certain “turning point” from which on any further movement would result in quickly adopting the optimal orientation. At first sight it appears counterintuitive that a membrane-destined protein would face a certain resistance when immersed into the biomembrane (as implied by the insertion profile shown in Fig. 2). Biology, however, makes us think differently. MPs follow a different route to end up at the biomembrane [27]. Only a small minority of MPs become operational via simple ribosomal release into the cytosol followed by passive or assisted transport and integration into the biomembrane [28–30]. Much more common is the detour via the translocon [31], a strongly conserved multi-component complex [32], that guides MPs eventually into the bilayer via lateral partitioning from the already membrane-embedded translocon [33]. Thus, the biological essence of a MP is correctly reproduced from an insertion profile of the type shown in Fig. 2. Partial term analysis of the ΔG^{env} profile shown in Fig. 2 highlights the determining role of polarization and cavitation. Dispersion seems to be less decisive for this process. Sensitivity with respect to conformational flexibility has been partially addressed by repeating the above experiment but using averages over a small data set of 35 individual conformations (the latter obtained from a short MD run). Corresponding data are shown in Fig. 1 of Supplementary material. While the overall variation of individual terms is small and main features of the single point evaluation shown in Fig. 2 are recovered, there is a certain reduction of free energy gain observable at the midpoint position of MP integration.

3.3. Different orientations of a MP fragment probed at the top layer of the biomembrane reveal one favoured conformation that is identical to the experimentally observed one

The Major Coat Protein of M13-Bacteriophages has been reported to attain a flail-like structure [34]. One branch is inserted into the membrane similar to a TM-helix, while the other part attaches flat on top of the lipid bilayer (see Fig. 3). This specific arrangement led to a hypothetical model of coat protein assembly. For the present purpose the TM-domain (green to blue stretch in Fig. 3) is cut off and not included in any calculation. The environmental effect, ΔG^{env} (see Eq. (1)), is estimated via a multiple continua approach where the N-terminal α -helical fragment is rotated around its own axis and various specific orientations are studied. This means, essentially, varying re-assignment of helix residues to the AQ or PH domain, respectively. The rotation profile is depicted in Fig. 3. Little change is seen in the cavitation and dispersion terms and the entire effect becomes an effective function of the polarization term. A single conformation is projected out as the energetically preferred one. This favoured conformation corresponds to the experimentally observed one (see Supplementary material Table IV). Biologically this arrangement meets two goals at the same time. On the one hand, it prevents the N-terminal branch to integrate deeper into the membrane interior, while on the other hand it allows great—but directed—flexibility to the N-terminal α -helix as is probably required for proper coat protein assembly [35].

3.4. The biomembrane stabilizes the relative TM orientation in the zeta-zeta dimer

Activation of the T-cell receptor is a complex interplay of many components. Among them is the dimerization of the zeta TM do-

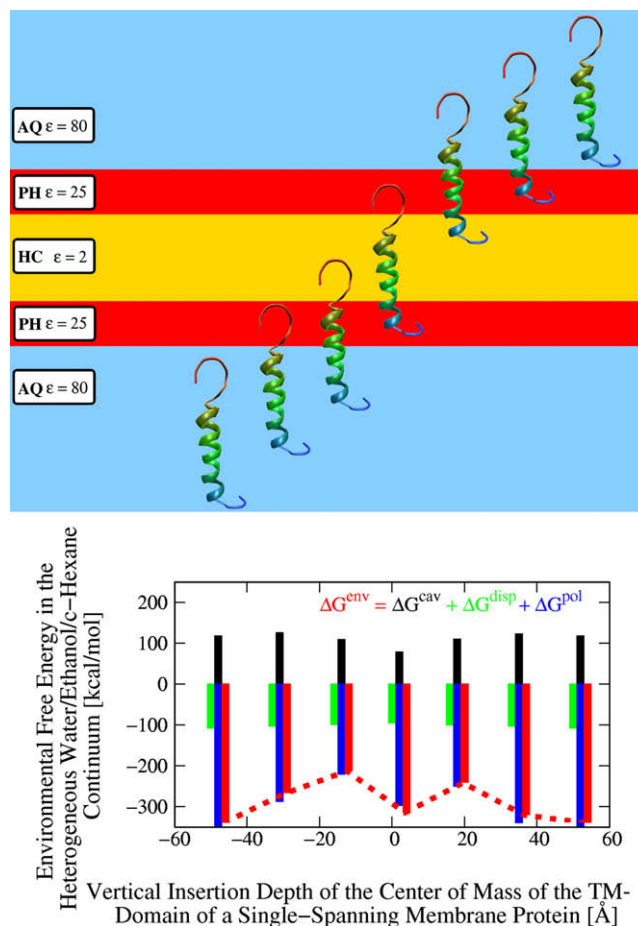


Fig. 2. Insertion of a single-spanning α -helical protein. The NMR structure of Sarcolipin (N-terminus red, C-terminus blue, PDB-code 1JDM) was probed for seven positions along the membrane normal (AQ, water; PH, polar heads; and HC, hydrophobic core) using the multiple continua approach. The partial free energy contributions ΔG^{cav} (black bars), ΔG^{disp} (green bars), and ΔG^{pol} (blue bars) combine to the total environmental effect ΔG^{env} (red, dotted line). Both the positions in aqueous environment as well as a central, membrane-integrated state are stabilized by the polarization term.

mains [36]. Corresponding NMR studies of the zeta-zeta TM dimer have been carried out and an activation model was proposed. Similar to other NMR studies on TM dimerization [37,38] specific interactions between the two TM domains are identified as the driving force (i.e. the aspartic acid pair [36]). The multiple continua approach allows the TM-dimer to be analyzed from a different perspective. Only the stabilizing/de-stabilizing effect of the membranous environment can be examined without considering any specific interactions between the two TM domains. Particularly interesting is the question whether different parts of the TM-helices are preferentially exposed outwards where they would face the membranous environment or rather prefer to be oriented inwards where they would become covered in the dimer-interface domain. Probing a set of model dimer structures should help to address this point. Therefore we first break the disulfide bond between the two CYS₂ residues of both TM domains to facilitate free individual rotations around either TM axis. Then we separate the TM domains into individual structures and rotate the first TM by 105° around its own TM axis (deviating from the NMR geometry). What follows is a series of corresponding rotations of the second TM domain by 0°, 105°, 210° and 315° (also deviating from the NMR geometry). Any pair of individual rotations is followed by re-combination to a dimer structure (at changed relative orientation of the two TM

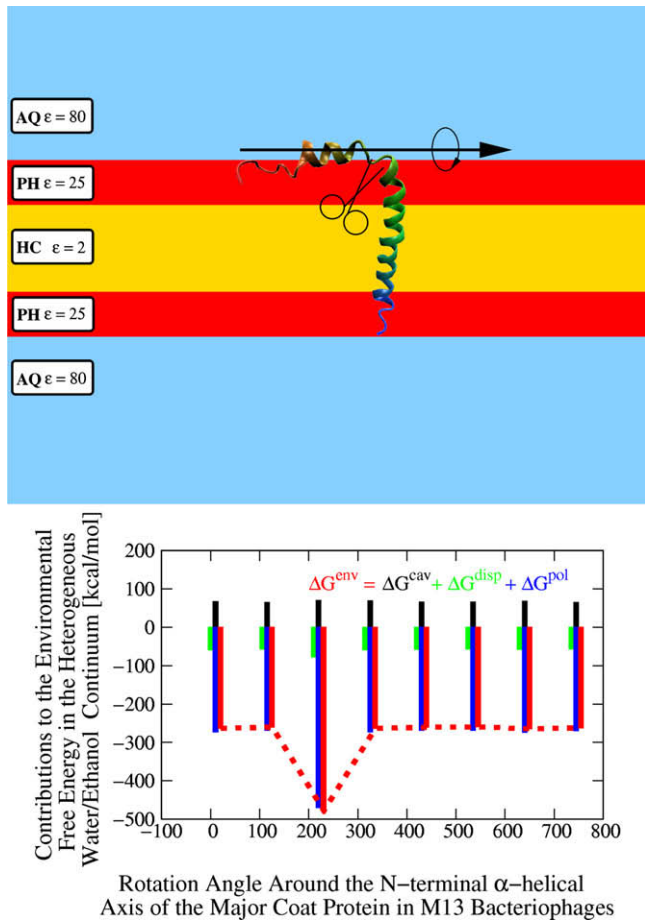


Fig. 3. Planar orientation of the membrane–water interface. The N-terminal α -helical fragment of the Major Coat Protein of bacteriophage M13 (N-terminus red, C-terminus blue, PDB-code 2CPS) is probed for various rotation angles θ at the top-layer of the biomembrane (AQ, water; PH, polar heads; and HC hydrophobic core). The TM domain (cut-off as indicated) was not considered for this analysis. The partial free energy contributions ΔG^{cav} (black bars), ΔG^{disp} (green bars), and ΔG^{pol} (blue bars) combine to the total environmental effect ΔG^{env} (red, dotted line). The preferred orientation ($\theta = 210^\circ$) matches the one observed in the NMR structure.

domains) and molecular mechanics minimization of the resulting geometry (2000 steps steepest descent/conjugate gradient). The latter is necessary to clear the model-built dimer structure of arising steric conflicts. Further incremental rotations of the first TM domain by another 105° combined with the above-mentioned corresponding rotations of the second TM domain will complete the cycle of geometrical transformations. Eventually a set of 16 hypothetical conformations of the zeta–zeta TM dimer will have been constructed and visually inspected. Note that the 0,0 conformer will represent the original NMR structure. Note further, that a rotation of 315° in the α -helical world means having gone back to the original conformation (1–4 interaction in the helix backbone). Each of these 16 conformations will be considered within the multiple continua approach and results are summarized in Fig. 4. All identified minima in the environmental free energy profile involve rotation angles of either 0° or 315° (see Fig. 4), hence correspond to the original NMR structure. In other words, the biomembrane itself drives the relative arrangement of the two TM domains into its optimal state. A detailed compilation of the data shown in Fig. 4 is provided in the Supplementary material Table V. It is interesting to re-identify the NMR structure via such purely theoretical considerations. However, the in vivo formation of the zeta–zeta dimer will be largely determined from the formation of the disulfide bond between the CYS₂ residues on the TM domains. Once the disulfide

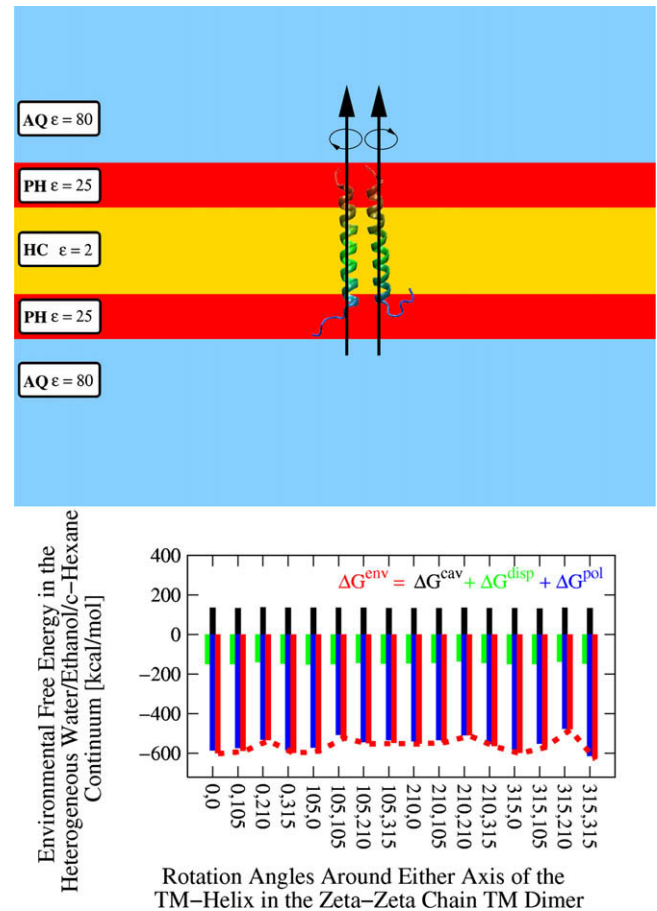


Fig. 4. Relative orientation of two transmembrane-helices. The NMR structure of the TM-dimer in the zeta–zeta complex of the T-cell receptor (N-terminus red, C-terminus blue, PDB-code 2HAC) were rotated independently by 105° increments around their helical axes. The steric conflicts for some of the orientations were removed before computing the environmental free energy by the multiple continua approach. The partial free energy contributions ΔG^{cav} (black bars), ΔG^{disp} (green bars), and ΔG^{pol} (blue bars) combine to the total environmental effect ΔG^{env} (red, dotted line). All the four minima in the scan involve rotation angles of 0° or 315° and thus refer to the original NMR structure.

bridge is established it will tether together the TM-helices at the N-terminal end and bring the two conserved ASP₆ residues into close proximity leaving little conformational freedom to the rest of the zeta–zeta TM dimer. When estimating the environmental contribution to the dimerization process, i.e. $\Delta \Delta G^{\text{env}}$ (dimer-TM₁-TM₂), small but positively signed energies are obtained, hence this effect is not the sole driving force for the process (see Supplementary material Fig. II). A signalling-defunct double mutant (D2A D2A) does not reveal significant differences to the wt when analyzed in a similar manner (see Supplementary material Fig. II). While for the present problem rigid rotations followed by structural optimizations appear to be sufficient, a more rigorous account of the conformational flexibility will be necessary for more complex problems to be studied in a similar manner. This could be achieved from carrying out MD simulations first, saving a series of snapshot structures along the trajectory and post-processing the latter with a series of individual multiple continua calculations.

3.5. The multiple continua approach achieves semi-quantitative levels of accuracy

Assessment of the quantitative accuracy of the multiple continua approach was done by comparing results to high level

molecular dynamics data. We use the extensive work of Berendsen and coworkers [10–12]. The passage of small molecules across the bilayer is studied using the multiple continua approach and comparing results to the molecular dynamics simulations of Berendsen and coworkers. Fig. 5 shows the relative free energy profile of a single molecule of water crossing the biomembrane. Owing to the fact that the boundary of the substance in question defines the assignment to a particular domain, small molecules like water will experience a large number of “degenerate” positions on their path across the bilayer. In fact, such a simplistic model offers only 5 different positions to probe small molecules for varying environmental conditions, i.e. residing entirely in the AQ, PH or HC domains, or at the interface between the AQ and PH domains, or at the interface between the PH and HC domains. The profile will be perfectly symmetric with respect to the midplane of the bilayer. Thus only the initial five data points (red squares) in Fig. 5 represent distinguishable multiple continua calculations. In spite of all these simplifying conditions rather close agreement between the multiple continua approach and the much more elaborate molecular dynamics data of Berendsen and coworkers is observed, both in qualitative as well as quantitative terms. Similar results are obtained for the same type of analysis of small molecules NH_3 and O_2 (see Supplementary material Figs. III and IV). Partial term analysis of the permeation profiles reveals a dominating contribution of the cavitation and polarization terms but rather static behaviour of dispersion. The latter, however, is the sole counter-balancing effect in the case of

O_2 passage (see Supplementary material Fig. IV), hence deserves its classification as principal constituent.

3.6. Conclusion

A series of case studies based on a simple biomembrane model renders the underlying physical approximation of the latter reasonable. The PCM-like [18] composition proves to be valuable for a deeper analytic insight into how different types of physical interaction work together. Improvements in the continuum description of solvated matter have set the stage for more complex problems to be addressed. All cases studied within this present work point towards an active role of the biomembrane in defining location and relative orientation of biomolecules in the bilayer.

Acknowledgements

This work was supported in part by the Project HPC-EUROPA++ (RII3-CT-2003-506079) funded by the European Community – Research Infrastructure Action under the programme FP6 “Structuring the European Research Area”. Generous access to large scale computational resources was granted within the Austrian Grid initiative and is gratefully acknowledged.

Appendix A. Supplementary data

Supplementary data associated with this article can be found, in the online version, at doi:10.1016/j.febslet.2009.04.040.

References

- [1] Wu, C.C. and Yates III, J.R. (2003) The application of mass spectrometry to membrane proteomics. *Nat. Biotechnol.* 21, 262–267.
- [2] White, S.H. and Wimley, W.C. (1998) Hydrophobic interactions of peptides with membrane interfaces. *Biochim. Biophys. Acta* 1376, 339–352.
- [3] Ashcroft, R.G., Coster, H.G.L. and Smith, J.R. (1981) The molecular organization of biomolecular lipid membranes. The dielectric structure of the hydrophilic/hydrophobic interface. *Biochim. Biophys. Acta* 643, 191–204.
- [4] Honig, B.H., Hubbell, W.L. and Flewelling, R.F. (1986) Electrostatic interactions in membranes and proteins. *Annu. Rev. Biophys. Biophys. Chem.* 15, 163–193.
- [5] Parsegian, A. (1969) Energy of an ion crossing a low dielectric membrane: solutions to four relevant electrostatic problems. *Nature* 221, 844–846.
- [6] Bechor, D. and Ben-Tal, N. (2001) Implicit solvent model studies of the interactions of the influenza hemagglutinin fusion peptide with lipid bilayers. *Biophys. J.* 80, 643–655.
- [7] Ben-Tal, N., Ben-Shaul, A., Nicholls, A. and Honig, B.H. (1996) Free-energy determinants of α -helix insertion into lipid bilayers. *Biophys. J.* 70, 1803–1812.
- [8] Tanizaki, S. and Feig, M. (2005) A generalized Born formalism for heterogeneous dielectric environments: application to the implicit modeling of biological membranes. *J. Chem. Phys.* 122, 124706.
- [9] Im, W., Feig, M. and Brooks III, C.L. (2003) An implicit membrane generalized Born theory for the study of structure, stability and interactions of membrane proteins. *Biophys. J.* 85, 2900–2918.
- [10] Egberts, E., Marrink, S.J. and Berendsen, H.C.J. (1994) Molecular dynamics simulation of a phospholipid membrane. *Eur. Biophys. J.* 22, 423–436.
- [11] Marrink, S.J. and Berendsen, H.C.J. (1994) Simulation of water transport through a lipid membrane. *J. Phys. Chem.* 98, 4155–4168.
- [12] Marrink, S.J. and Berendsen, H.C.J. (1996) Permeation process of small molecules across lipid membranes studied by molecular dynamics simulations. *J. Phys. Chem.* 100, 16729–16738.
- [13] Jordan, P.C. (1981) Energy barriers for passage of ions through channels. Exact solution of two electrostatic problem. *Biophys. Chem.* 13, 203–212.
- [14] Kessel, A., Cafiso, D.S. and Ben-Tal, N. (2000) Continuum solvent model calculations of alamethicin-membrane interactions: thermodynamic aspects. *Biophys. J.* 78, 571–583.
- [15] von Kitzing, E. and Soumpasis, D.M. (1996) Electrostatics of a simple membrane model using Green’s functions formalism. *Biophys. J.* 71, 795–810.
- [16] Feynman, R.P. (1963) *The Feynman Lectures on Physics*, Addison Wesley, Reading, MA.
- [17] Kar, P., Seel, M., Hansmann, U.H.E. and Höfinger, S. (2007) Dispersion terms and analysis of size- and charge dependence in an enhanced Poisson–Boltzmann approach. *J. Phys. Chem. B* 111, 8910–8918.
- [18] Tomasi, J., Mennucci, B. and Cammi, R. (2005) Quantum mechanical continuum solvation models. *Chem. Rev.* 105, 2999–3094.

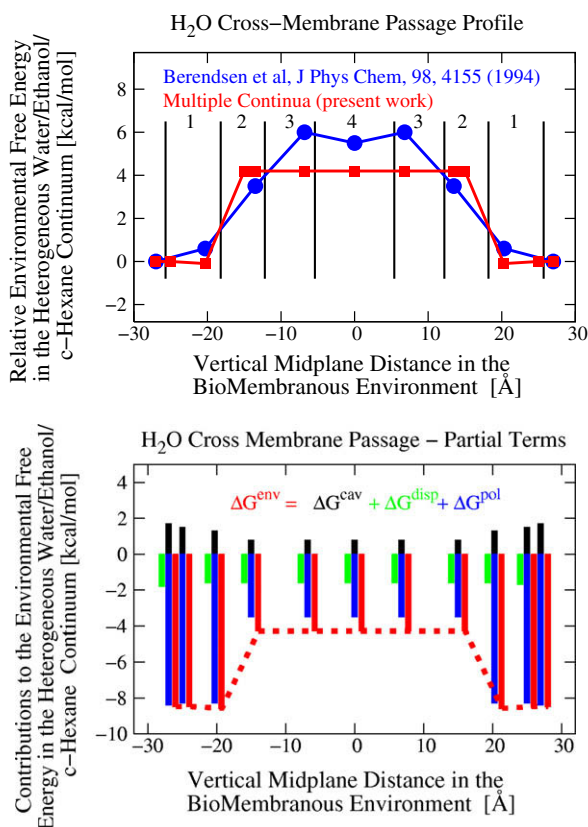


Fig. 5. Passage of a single water molecule across the biomembrane. A single molecule of water is probed at various positions along the membrane normal. Relative free energies of environmental stabilization, $\Delta\Delta G^{\text{env}}$, are computed using the multiple continua model (reference is solvation in pure water, ΔG^{aq} , i.e. outermost data points in lower panel). The resulting profile is compared to the data reported by Berendsen et al. [11]. Despite its simplistic nature the multiple continua model resembles the much more elaborate MD data rather closely.

- [19] Höfinger, S. (2005) Solving the Poisson–Boltzmann equation with the specialized computer chip MD-GRAPe-2. *J. Comput. Chem.* 26, 1148–1154.
- [20] Höfinger, S. and Zerbetto, F. (2005) Simple models for hydrophobic hydration. *Chem. Soc. Rev.* 34, 1012–1020.
- [21] Zauhar, R.J. and Morgan, R.S. (1985) A new method for computing the macromolecular electric potential. *J. Mol. Biol.* 186, 815–820.
- [22] Tusnányi, G.E., Dosztányi, Zs. and Simon, I. (2004) Transmembrane proteins in protein data bank: identification and classification. *Bioinformatics* 20, 2964–2972 (Online database: Protein Data Bank of Transmembrane Proteins (2008) Institute of Enzymology, Budapest, Hungary. <<http://pdbtm.enzim.hu/?m=sform>>).
- [23] Case, D.A., Cheatham, T.E., Darden, T., Gohlke, H., Luo, R., Merz Jr., K.M., Onuvriev, A., Simmerling, C., Wang, B. and Woods, R. (2005) The Amber biomolecular simulation programs. *J. Comput. Chem.* 26, 1668–1688. AMBER Home Page (2008). <<http://ambermd.org>>.
- [24] Wimley, W.C. and White, S.H. (1996) Experimentally determined hydrophobicity scale for proteins at membrane interfaces. *Nat. Struct. Biol.* 3, 842–848.
- [25] Ponder, J.W. (2004) TINKER Software Tools for Molecular Design Version 4.2 Copyright ©1990–2004 by Jay William Ponder.
- [26] Mascioni, A., Karim, C., Barany, G., Thomas, D.D. and Veglia, G. (2002) Structure and orientation of sarcolipin in lipid environments. *Biochemistry* 41, 475–482.
- [27] Johnson, A.E. and van Waes, M.A. (1999) The translocon: a dynamic gateway at the ER membrane. *Annu. Rev. Cell. Dev. Biol.* 15, 799–842.
- [28] Abell, B.M., Rabu, C., Leznicki, P., Young, J.C. and High, S. (2007) Post-translational integration of tail-anchored proteins is facilitated by defined molecular chaperons. *J. Cell. Sci.* 120, 1743–1751.
- [29] Zimmer, J., Nam, Y. and Rapoport, T.A. (2008) Structure of a complex of the ATPase SecA and the protein-translocation channel. *Nature* 455, 936–943.
- [30] Tsukazaki, T., Mori, H., Fukai, S., Ishitani, R., Mori, T., Dohmae, N., Perederina, A., Sugita, Y., Vassilyev, D.G., Ito, K. and Nureki, O. (2008) Conformational transition of Sec machinery inferred from bacterial SecYE structures. *Nature* 455, 988–991.
- [31] Blobel, G. (1999). Protein Targeting. Copyright, The Nobel Foundation 1999, Nobel Lecture, Physiology.
- [32] van den Berg, B., Clemons Jr., W.M., Collinson, I., Modis, Y., Hartmann, E., Harrison, S.C. and Rapoport, T.A. (2004) X-ray structure of a protein-conducting channel. *Nature* 427, 36–44.
- [33] White, S.H. (2007) Membrane protein insertion: the biophysics nexus. *J. Gen. Physiol.* 129, 363–369.
- [34] Papavoine, C.H.M., Christiaans, B.E.C., Folmer, R.H.A., Konings, R.N.H. and Hilbers, K.W. (1998) Solution structure of the M13 Major coat protein in detergent micelles: a basis for a model of phage assembly involving specific residues. *J. Mol. Biol.* 282, 401–419.
- [35] Williams, K.A., Glibowicka, M., Li, Z., Li, H., Khan, A.R., Chen, Y.M.Y., Wang, J., Marvin, D.A. and Deber, C.M. (1995) Packing of coat protein amphipathic and transmembrane helices in filamentous bacteriophage m13: role of small residues in protein oligomerization. *J. Mol. Biol.* 252, 6–14.
- [36] Call, M.E., Schnell, J.R., Xu, C., Lutz, R.A., Chou, J.J. and Wucherpennig, K.W. (2006) The structure of the tetazeta transmembrane dimer reveals features essential for its assembly with the T cell receptor. *Cell* 127, 355–368.
- [37] Gratkowski, H., Lear, J.D. and DeGrado, W.F. (2001) Polar side chains drive the association of model transmembrane peptides. *Proc. Natl. Acad. Sci. USA* 98, 880885.
- [38] Zhou, F.X., Merianos, H.J., Brunger, A.T. and Engelman, D.M. (2001) Polar residues drive association of polyleucine transmembrane helices. *Proc. Natl. Acad. Sci. USA* 98, 22502255.